Low and high enthalpy shock wave /boundary layer interactions around cylinder-flare models

Bruno Chanetz

Fundamental and Experimental Aerodynamics Department – ONERA 92190 Meudon, France
Associate Professor at the University of Versailles Saint-Quentin en Yvelines

SUMMARY

The paper describes four test-cases around the same configuration type : a hollow cylinder flare model. The first three test-cases are relative to cold hypersonic and the fourth one to hot hypersonic :

- a purely laminar low enthalpy interaction performed at Mach 9.92 ;
- a transitional low enthalpy interaction performed at Mach 5;
- a fully low enthalpy turbulent interaction performed at Mach 5 ;
- a high enthalpy interaction performed at Mach 9.4.

1) INTRODUCTION

In spite of the spectacular progress in CFD there is still a strong need to validate the computer codes by comparison with experiments. For reason of calculating cost, it is better to consider two-dimensional configurations. Since a truly two-dimensional configuration is difficult to reach in a wind tunnel, because of the starting constraints which forbid the use of large spanwise models, these experiments have been executed on axisymmetric configurations. The experiments here presented issued from the data bank [1] of the fundamental and experimental aerodynamics department at ONERA Meudon are precious to help in the development of reliable and accurate codes.

The paper provides four test-cases around the same model shape : a hollow cylinder flare model. In such a model are avoided the side effects due to the finite span of any two-dimensional arrangement but the mathematical simplicity of a two dimensions space is kept. An axisymmetrical configuration facilitates a rigorous numerical study with the present computational capabilities. These models relative to academic configurations have been chosen in order to simulate the shock wave/boundary layer interactions occurring on flap. Indeed shock wave/boundary-layer interactions in hypersonic flows may have major consequences on thermal loads, especially if the shock is strong enough to induce separation. Furthermore the heat-flux density levels in the interaction region strongly depend on the nature, laminar, transitional or turbulent of the boundary-layer and the phenomena are still more difficult when reacting gas hypersonic is considered. Therefore this paper presents laminar, transitional and turbulent shock-wave boundary layer interactions in cold hypersonic and also such an interaction in hot hypersonic.

2) LOW ENTHALPY LAMINAR INTERACTION LAMINAR INTERACTION

2.1) aim of the study and conditions of experiment

Entirely laminar flows have been realized in the low Reynolds number R5Ch wind tunnel whose operating conditions are: Mach number: M_0 = 9.92, stagnation temperature: T_{st} = 1050K, stagnation pressure: p_{st} = 2.5×10^5Pa. The unit Reynolds number (186,000m^{-1}) is sufficiently low to warrant a laminar regime throughout the interaction domain.

The model is constituted by a hollow cylinder, with a sharp leading edge, followed by a flare terminated by a cylindrical part. The model has a total length of 170mm, the reference length, based on the distance between the sharp leading edge and the beginning of the 30° flare, is equal to *L* = 101.7mm The outer cylinder diameter is equal to 65mm whereas the inner one is equal to 0.045 m. The Reynolds number based on the reference length is equal to Re_L = 18,600.
The flow has been visualised thanks to Electron Beam Fluorescence (EBF) technique [2]. The wall pressure measurements were executed with variable reluctance differential transducers and the heat fluxes determined from the surface temperature rise by using platinum films. In addition to wall measurements density, specific mass measurements were performed by the electron beam X-ray technique [2].

The present results are compared with calculated data issued from three different solvers [3] :
- a Navier-Stokes research solver from ONERA : NASCA (finite volumes)
- a Navier-Stokes code from DLR : FLOW (finite elements)
- a Direct Simulation Monte-Carlo solver from NASA Langley : DSMC

2.2) presentation of the results

Figure 1 shows an EBF visualisation where the attached shock-wave at the sharp leading edge and the separation shock-wave are evidenced. These two shocks converge and interfere above the end of the flare. Three density profiles were probed at X/L = 0.3, X/L = 0.6 and X/L = 0.76.

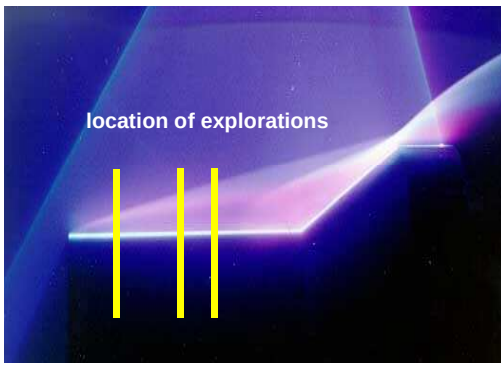

Figure 1 : Electron Beam Fluorescence visualization (low enthalpy laminar interaction)

Wall pressure measurements are transformed into a pressure coefficient : $C_p = 2\,(p/p_0 - 1)/\,\gamma M_o^2$ where M_o and p_o are the upstream Mach number and upstream static pressure.

Figure 2a presents the longitudinal evolution of the pressure coefficient measured on the hollow cylinder-flare model for ten runs. The pressure coefficient is decreasing slowly on the upstream part of the cylinder till abscissa X/L = 0.7. This decrease is followed by a two step compression. A first compression is due to the separation process and a second compression, far more important, occurs during reattachment. The Navier-Stokes codes give a fair prediction of the wall pressure distribution in the separated flow, whereas the DSMC code highly over-predicts the peak pressure.

Wall heat-flux densities q_w are transformed into a thermal coefficient $h = q_w/(T_{st} - T_w)(W/m^2/K)$, where T_{st} is the stagnation temperature and T_w is the wall temperature at the beginning of the run. Then the results are expressed in a dimensionless form by introducing the Stanton number defined by :
$St = h/\rho_0\, U_0\, C_p$ where C_p = 1004.5 J/kg/K and ρ_0 and U_0 are inferred from the upstream conditions.

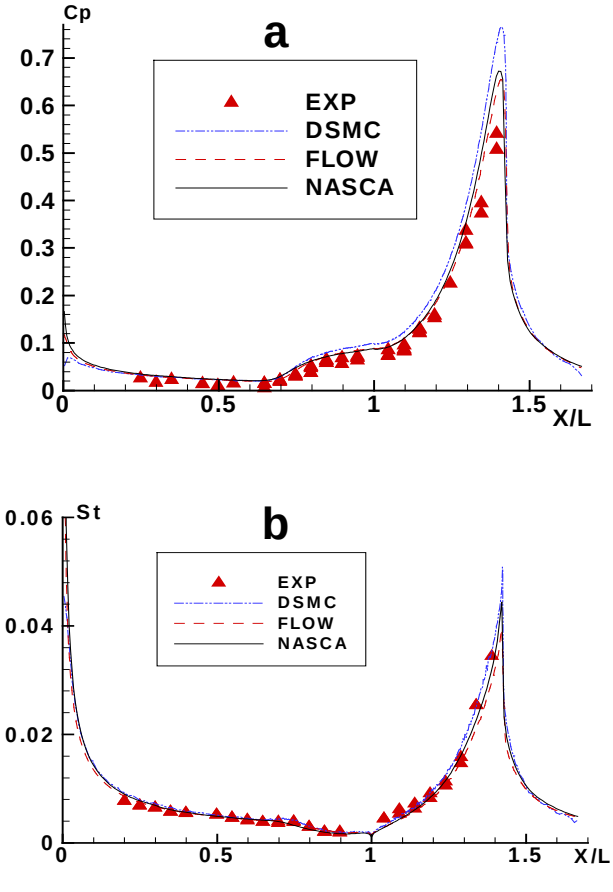

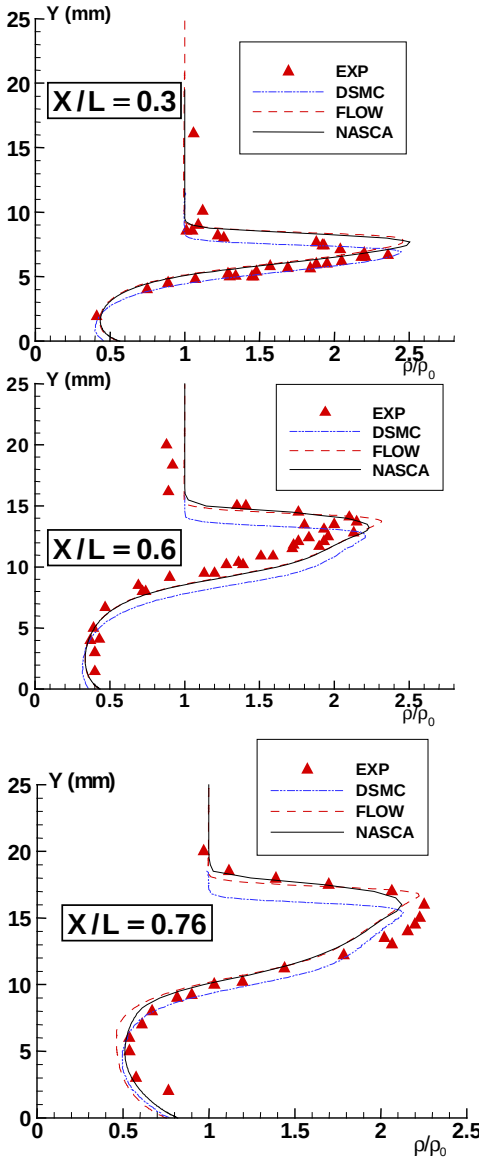

Figure 2 : Surface measurements a: pressure, b: heat-transfer (low enthalpy laminar interaction)

Figure 3 : Density profile measurements (low enthalpy laminar interaction)

Figure 2b presents the evolution of the Stanton number along the cylinder flare. The heat-flux decreases along the cylinder in the upstream part, where the flow is governed by the viscous interaction effects emanating from the leading edge. Further downstream, the evolution is characteristic of a laminar interaction with a large boundary layer separation : after a first decrease in the heat-flux evolution beginning at the abscissa where the separation begins (X/L = 0.77), this flux increases on the flare, with an enforcement of this increase from the reattachment point. .

Besides wall measurements, field quantities have been measured around the model. As shown in the figure 3, the density profile at *X/L* = 0.3 is located forward of the separation line. At this station, the increase of density is due to the shock generated by the sharp leading edge. The DSMC calculation is here in excellent agreement with experiment. For the profiles at *X/L* = 0.6 the best predictions of the radial shock location is given by the Navier-Stokes codes. The profiles at *X/L* = 0.76 present the same tendencies.

3) LOW ENTHALPY TRANSITIONAL INTERACTION

3.1) conditions of the experiment

An hollow cylinder-flare model was used. It is composed of a first cylinder with sharp leading edge, of D=131 mm diameter and L = 252 mm length, followed by a 15° conical flare (length 101.4 mm). The flare itself is followed by a 50 mm long cylindrical extension in order to minimize the base flow influence on the interaction region. Total length of the model is 349 mm. The ONERA Meudon center R2Ch wind tunnel was used for the present experiments. R2Ch wind tunnel is a blow-down facility (test duration between 15 and 30 seconds) here equipped with a Mach 5 contoured axisymmetric nozzle. Upstream air is heated to a stagnation temperature T_{st} of approximately 500 K by streaming through a Joule effect heater. Stagnation pressure p_{st} can be adjusted between 0.9×10^5 and 70×10^5 Pa. R2Ch wind tunnel is - as R5Ch - a cold hypersonic facility, in the sense that the stagnation temperature is raised to a level just sufficient to prevent air liquefaction during expansion in the nozzle. The present test has been performed for a stagnation pressure $p_{st}= 0.9\times10^5$ Pa, which corresponds to a Reynolds number $Re_L= 0.38\times10^6$ based on the reference length L.

For axi-symmetric configurations, the separation line is very sensitive to the model incidence and yaw angles. Great care was taken to control model setting in the flow by examining the surface flow with the help of viscous coating visualizations. This technique consists in projecting a mixture of lamp black and silicone oil, with a viscosity suited to the local skin friction level, onto the model before the test. The skin friction lines pattern establishing during the run allows to identify separation and reattachment lines, thus permitting to check the flow axial symmetry (see Fig. 4).

Pressure and heat-fluxes have been measured by mean of pressure transducers and heat-flux sensors.. The velocity field has been probed by two-component Laser Doppler Velocimetry (LDV). The boundary-layer was probed at different stations located upstream, inside and downstream of the interaction region. In the present case, the probe volume is a circular ellipsoid having a major axis of a few mm and a minor axis of 0.280 mm. The minimum probing distance to the wall was close to 0.4 mm. The uncertainty for LDV measurements inside the boundary layer is about 1 % of the maximum velocity modulus of the upstream external flow U_o (830 m/s). In the external, high velocity flow, due to the particle drag, this uncertainty rises up to 5 % of U_0.

3.2) Presentation of the results [4]

The surface flow visualization represented in the figure 4 shows the separation (at X/L=0.73) and reattachment lines (at X/L=1.23).

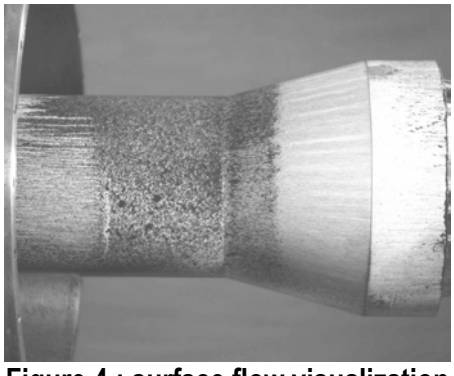

Figure 4 : surface flow visualization (low enthalpy transitional interaction)

The location of separation well agrees with that predicted by a laminar calculation performed with the ONERA-NASCA solver.

Wall pressure and heat-flux distributions measured in the R2Ch wind tunnel are compared in the figures 5 and 6 with the calculated values obtained with the NASCA code for laminar conditions. Concerning the separation point, a good agreement is obtained between experiment and calculation. The pressure level in the reverse flow zone is also well predicted by the calculation. As far as the heat-flux distribution is concerned, a rough agreement between calculation and experiment is observed until X/L=1. However, the experimental heat-flux peak following the reattachment is about 2.5 times higher than the laminar calculation. This result is in agreement with the well-known tendencies relative to the transitional thermal loads, which are larger than the laminar ones and even larger than the turbulent ones as it has been also proven by experiments performed at Onera [4] for an identical Reynolds number in natural transition or with triggered transition

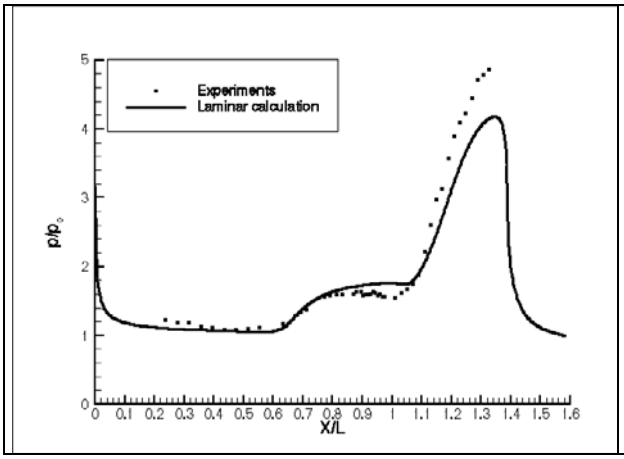

Figure 5 : Wall pressure distribution (low enthalpy transitional interaction)

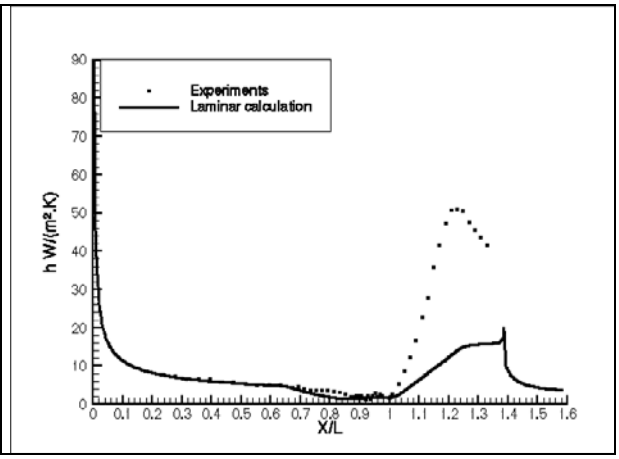

Figure 6: Wall heat-transfer distribution (low enthalpy transitional interaction)

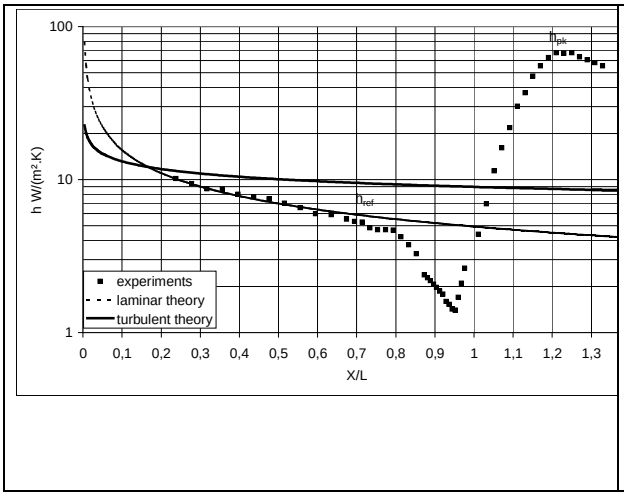

Figure 7: Wall heat-flux density distribution in semi-logarithm plot (low enthalpy transitional interaction)

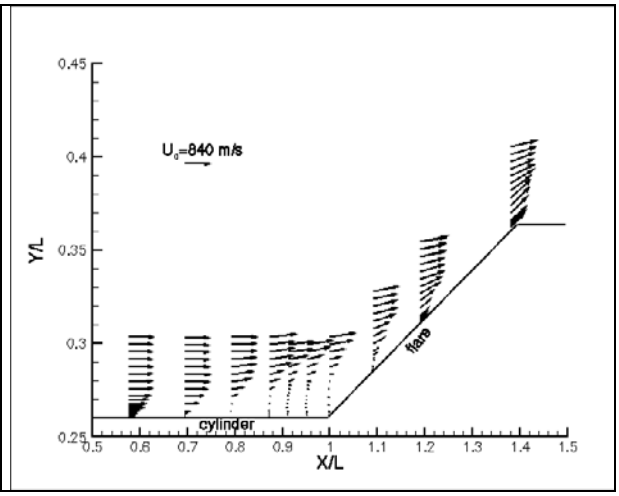

Figure 8 : LDV measurements (low enthalpy transitional interaction)

The semi-logarithmic plotting of the measured heat-flux density evolution in the figure 7 emphasizes the important decrease of heat-flux density in the separation region typical of laminar separation. The laminar and turbulent wall heat-fluxes calculated on a flat plate for the same stagnation conditions are added in the figure. Close agreement is observed between experiments and the laminar theory up to the point of separation, which confirms the laminar nature of separation.
Results of the LDV measurements are shown in the figure 8. In this case, the separation point location is evaluated at X/L=0.69 according to the oil-flow visualization shown in the figure 4. The incompressible shape factor for the first boundary-layer velocity profile located at X/L=0.57 is equal to H_i=2.57. This value is characteristic of a laminar boundary layer. At X/L=0.69 just upstream of the separation abscissa, the incompressible shape factor is still equal to H_i=2.59 confirming the laminar character of the flow upstream of separation.

4) LOW ENTHALPY TURBULENT INTERACTION

4.1) Conditions of the experiments

This test-case [5] was performed in the R2Ch wind tunnel already described (see § 3.1). The present experiment was performed for the following conditions at M_0 = 5 : stagnation pressure p_{st} = 35×10^5 Pa and stagnation temperature T_{st} = 500 K. These free stream conditions correspond to a unit Reynolds number equal to 44.1 x 10^6 m^{-1}. The model is constituted by a hollow cylinder with an external diameter of 131 mm and an internal diameter of 106 mm. The leading edge is sharp with an interior angle of 10°. A 35° flare is mounted 250 mm downstream of the cylinder. The total length of the model is equal to 300 mm. The Reynolds number based on the reference length L = 0.25 m is equal to Re_L = 11 10^6 and was sufficiently high to insure a natural fully turbulent boundary layer well upstream of the cylinder-flare junction.

4.2) Presentation of the results

The wall pressure distribution is given in the figure 9. The pressure p measured at the wall is divided by the free stream infinite pressure p_0. Along the cylinder part p is nearly equal to p_0 (p/p_0 = 1) till abscissa X/L = 0.9, where it increases strongly, which is the sign of a turbulent separation. This feature is confirmed by the heat-flux distribution presented in the figure 10, where an increase of the thermal coefficient is observed between X/L = 0.4 and X/L = 0.5.

Thus the end of transition took place at X/L = 0,5 , 125 mm downstream of the cylinder edge, i.e; in the middle of the cylinder part. Then a separation of the boundary layer occurs before the flare in fully turbulent regime. Heat transfer increases, which is typical of a separation onset in turbulent regime. This experiment constitutes an interesting test-case to test turbulence models.

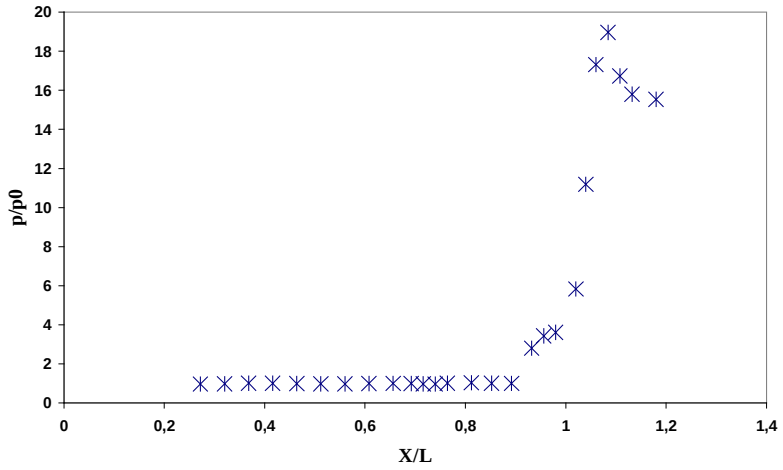

Figure 9 : Wall pressure distribution (low enthalpy turbulent interaction)

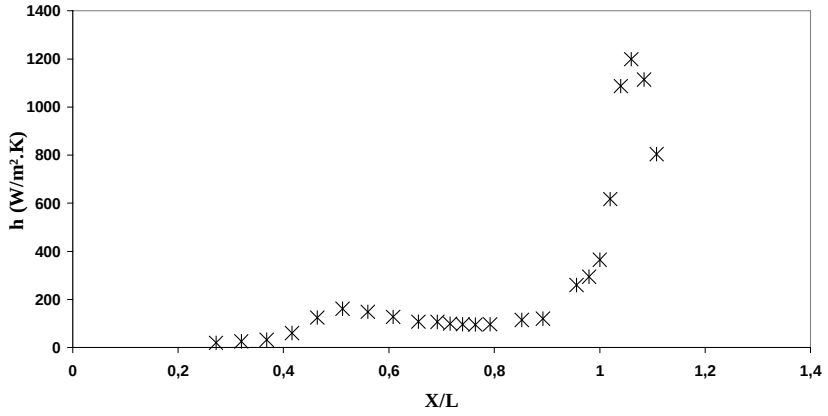

Figure 10 : Wall heat-transfer distribution (low enthalpy turbulent interaction)

5) HIGH ENTHALPY INTERACTION

5.1) Conditions of the experiments

This test-case was also performed with a cylinder flare geometry composed by a hollow cylinder with a sharp leading edge, an external diameter of 0.15 m, and a length L = 0.2 m, followed by a 35° conical flare, whose length is 0.067 m) and an additional cylindrical extension, which is 0.033 m long, set to inhibit the effects of the base flow on the interaction region. To measure the pressure distribution the model was equipped with DRUCK FDCR-42 transducers , in particular, 22 pressure taps are located along an upper generating line. To check the correct position of the model inside the chamber, the model was equipped with four additional control taps located symmetrically along the generating line at ± 90° with respect to the original one. To measure the heat flux, the model was equipped with 22 thermocouples located along an upper generating line at 180° from the upper generating line and at the same streamwise positions (of the pressure taps).

Two runs have been performed at quite the same conditions. One in air and another with Nitrogen in order to qualify an eventual effect of dissociation. In the conditions of the run with air, Onera-F4 high-

enthalpy wind tunnel flow conditions at the nozzle exit are M_∞ = 9.4, Re_∞/m = 1.15 10^5 , T_∞ = 522 K and V_∞ = 4318 m/s, thus corresponding to a stagnation pressure p_{st} = 230x10^5 Pa and a total enthalpy h_{st} = 9.93 MJ/kg.

5.2) presentation of the results

In order to compare with the other run performed with nitrogen, it is necessary to consider the good parameters. Indeed the run duration is comprised between 200 ms and 300 ms, but only the half of the duration is available for valuable measurements. During this duration, the stagnation conditions (pressure and enthalpy) are decreasing. In fact for each run, it is possible to consider more than one hundred different conditions. The comparison between air and nitrogen is interesting to evaluate the effect due to the dissociation, since with air the dissociation of O_2 molecules occurs at 2500 k, whereas with pure nitrogen the dissociation of N_2 occurs at 4000 K. In order to have a good comparison it has been demonstrated [6] that we have to consider the same stgnation enthalpy and the same global viscous interaction parameter $\underline{X} = M/(Re_L)^{0.5}$, this parameter inferred from the Pitot pressures measured at the nozzle exit. Thus the following conditions have been chosen :

- for the run 848 with air : p_{st} = 22,991,200 Pa ; h_{st}/rTa = 125.7 , $\underline{X}$ = 0.0627 ;
- for the run 849 with Nitrogen : p_{st} = 19,613,700 Pa ; h_{st}/rTa = 125.3 , $\underline{X}$ = 0.0648 ;

The longitudinal evolution of wall heat-flux density Φ expressed in W/m^2 is presented in the figure 11 and the longitudinal evolution of the pressure is presented in the figure 12 also in semi-logarithm plot. This presentation emphasizes the separation occurring before the ramp and characterized both by the slight decrease of heat-flux and the correlative increase of pressure. With air – represented with small squares - the separation point is found at X/L = 0.7 and with nitrogen – represented with small triangles – the separation point is found at X/L = 0.75. The difference is not very sensitive, but sufficient to evidence some dissociation effects, even if the stagnation enthalpy was not sufficient to dissociate more efficiently O_2 molecules. Nevertheless this study constitutes an interesting mean/high enthalpy test-case for the validation of Navier-Stokes solvers in thermo-chemical desequilibrium [7].

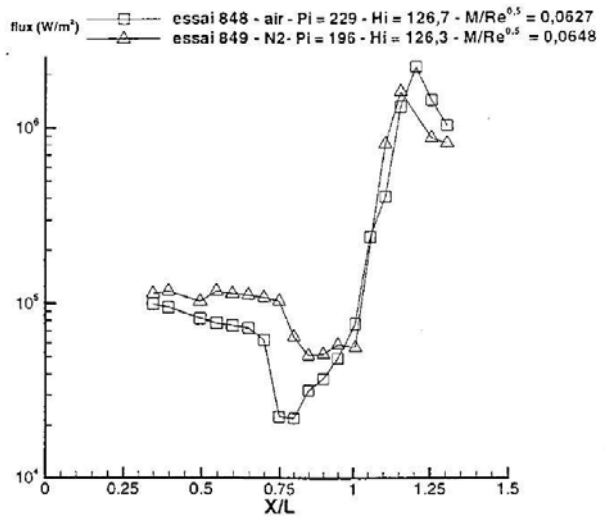

Figure 11 : Wall heat-transfer distribution (high enthalpy interaction)

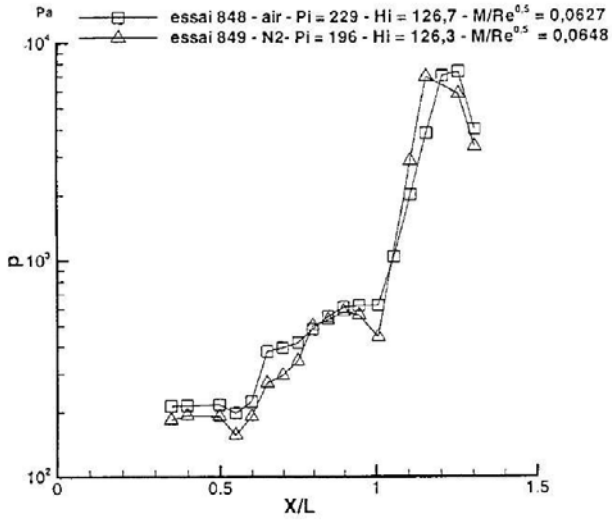

Figure 12 : Pressure distribution (high enthalpy interaction)

6) CONCLUSION

The first study presents an unquestionable shock wave/ boundary layer test-case in laminar flow, in order to validate numerical solvers without considering the complex problem of turbulence modelling.

The second one presents an unusual transitional shock wave/boundary layer interaction test-case. Indeed the problem of transitional interaction was often avoided because its calculation was too difficult. But precisely such interactions give rise to larger heat-fluxes at reattachment, even higher than those obtained in fully turbulent regime. Therefore this transitional well-documented test-case [4] achieved at Onera fills a blank in this domain. The third one completes the range in cold hypersonic since it is relative to a natural fully turbulent shock wave/boundary layer interaction, the transition occurring upstream of the separation. The fourth test-case is relative to high enthalpy hypersonic. The study performed in the F4 high-enthalpy wind tunnel has allowed a comparison between air and nitrogen for the same flow conditions. This comparison may be useful to validate Navier-Stokes solvers in thermo-chemical desequilibrium.

However a comparison restricted to the wall properties is in general insufficient to validate the most advanced predictive methods. In particular, information of the Mach number, temperature, density fields is essential to elucidate the cause of discrepancies affecting the wall distribution. In these conditions, the validation of computer codes requires well documented experiments providing not only wall quantities but also flow field measurements. It is remarkable that the breakthrough in our predictive capacity has been paralleled by spectacular developments in measurement techniques over approximately the same period. Thus two of the four test-cases presented have been carefully investigated thanks to non-intrusive diagnostic techniques : Laser Doppler velocimetry (LDV) to measure velocity and X-ray electron beam fluorescence (Xray-EBF) to measure density.

These four test-cases constitute a powerful data bank for hypersonic applications as far shock wave boundary layer interactions are concerned.

7) REFERENCES

[1] Benay, R. , Chanetz B. and Délery J.
Code verification :validation with respect to experimental data banks
Aerospace Science and Technology 7 (2003) 239-262.

[3] Gorchakova N., Chanetz B., Pot T., Bur R., Taran J.-P., Pigache D, Moss J., Schulte D., Kuznetsov L., Yarygin V.
Progress in Shock Wave- Boundary Layer Interaction Studies in Rarefied Hypersonic Flows Using Electron-Beam-Excited X-ray detection
AIAA Journal Vol. 40, n°4, pp. 593-598, April 2002 (ONERA TP n° 2002-76)

[3] Chanetz, B., Benay, R., Bousquet, J.-M., Bur, R., Pot, T., Grasso, F. and Moss, J.,
Experimental and Numerical Study of the Laminar Separation in Hypersonic Flow
Aerospace Science And Technology, No. 3, 1998, pp. 205-218

[4] Benay R ., Chanetz B., Mangin B., Vandomme L. and Perraud J.
Shock wave transitional boundary-layer interactions in hypersonic flow
AIAA journal, vol. 44, n°6, june 2006.

[5] Chanetz B.
ONERA hypersonic test-cases in the framework of Working Group 18th
"Hypersonic experimental and computational capability"
AGARD ADVISORY REPORT 319, vol. II (ONERA TP n° 1996-91)

[6] Sagnier Ph.
private communication

[7] Grasso F., Cuttica S., Ranuzzi G., Marini M. and Chanetz B.
Shock wave turbulent boundary layer interactions in non-equilibrium flows
AIAA journal vol. 39, n°11, november 2001 (Onera TP n° 2001-273)